FLUID SENSITIVITY OF ROCK PHYSICS PARAMETERS IN RESERVOIRS: QUANTITATIVE ANALYSIS

QINGCAI ZENG[1], YUQIAN GUO[2], REN JIANG[1], JING BA[3*], HONGDA MA[2] and JIONG LIU[4]

[1] *Research Institute of Petroleum Exploration and Development - Langfang, CNPC, Hebei 065007, P.R. China.*
[2] *CGG, 10300 Town Park Dr., Houston, TX 77072, U.S.A.*
[3] *School of Earth Sciences and Engineering, Hohai University, Nanjing 211100, P.R. China. jba@hhu.edu.cn*
[4] *Petroleum Exploration and Production Institute, SINOPEC, Beijing 100083, P.R. China.*

(Received May 27, 2016; revised version accepted December 13, 2016)

ABSTRACT

Zeng, Q., Guo, Y., Jiang, R., Ba, J., Ma, H. and Liu, J., 2017. Fluid sensitivity of rock physics parameters in reservoirs: Quantitative analysis. *Journal of Seismic Exploration*, 26: 125-140.

Pore fluid is an important factor affecting on reservoir properties. Generally, variations of elastic parameters reflect the changes of hydrocarbon saturation in rocks, which are meaningful for seismic identification of reservoir hydrocarbons. In this study, distribution features of the measured data are analyzed on the rock property crossplots, based on the relative variations of rock physics parameters between different fluid-saturation states, so that an evaluation methodology of effective fluid sensitivity indicator (EFSI) is presented to quantitatively analyze the influence of pore fluids on rock parameters. It is applied on the thirteen typical rock physics parameters based on the measured data from the carbonates of China. On the crossplots of the selected rock physics parameters with high EFSI values, reservoir rocks containing different types of fluid can be effectively discriminated.

KEY WORDS: Fluid Sensitivity Indicator (FSI), rock physics parameters, fluid identification, Effective Fluid Sensitivity Indicator (EFSI).

INTRODUCTION

Rock physical properties can be related to two basic aspects: dry rock matrix and pore fluid. Based on rock physics analysis, anomalous variations of rock properties which are relevant with fluid changes, can be extracted and exploited (Imhof, 2003). Rock elastic parameters respond to different pore fluids and can be used as an effective tool identifying oil/gas reservoirs.

0963-0651/17/$5.00

Pore fluid is an important factor affecting seismic responses of reservoirs (Batzle and Wang, 1992). Gray et al. (1999) derived the two attributes of AVO which are related to reservoir hydrocarbon. Keho et al. (2000, 2001) demonstrated the method of AVO holograms is more effective than AVO crossplots for identifying AVO anomalies. Computing method of fluid indicators from wide-azimuth PP-AVOA data was developed which can be used to establish fluid indicator estimates for gas fractures (Shaw and Sen, 2006). AVA modeling was introduced to analyze the effects of pore types and pore fluids on carbonate reservoir (Agersborg et al., 2008). Zhou and Hilterman (2007, 2010) evaluated the prediction capability of pore-fluid sensitivity analysis and compared the three AVO attributes from well-log data and seismic data for 183 reservoirs. According to their results, the basis of fluid sensitivity for the attributes is Poisson's impedance, and the same scale factor did not significantly affect the sensitivity of the attributes.

Zoeppritz equations for the continuity of displacement and stress give rise to the underlying emphasis on seismic velocity and density. The fluid factors and AVO attributes which are related to reservoir hydrocarbon can be derived from Zoeppritz equations (Gray et al., 1999). Normalizing the data for equivalent hydrocarbon-filled rocks against the fluid line might provide an optimum AVO indicator in the case that the effects of noise is low (Simm et al., 2000).

Fluid sensitivity identification factors have been proposed for the purpose of identifying fluid anomalies in in-situ rocks. Smith and Sutherland (1996) studied the method of fluid factors compared with the other AVO parameters based on measurements from 25 datasets (Castagna and Smith, 1994), and showed that fluid factor could help to distinguish gas sands from wetsands.

Fluid factors related to P-S-wave reflectivities and impedances were applied to sandstone sediment to indicate gas reservoir (Fatti et al., 1994). Generally, gas-saturated sandstone layers have a lower Poisson's ratio than that of brine-saturated layers (Ostrander, 1982). The rock physics parameters λ (Lamé constant) - μ (shear modulus) - ρ (density) method was first presented for identifying fluid anomalies by Goodway et al. (1997). Smith (2000, 2003) supported Gary's points by comparing the fluid factors with reflectivity attributes which are derived from λ, μ and ρ. Goodway (2001) introduced the fluid factor of $\lambda\rho$, and his study shows a distinguished potential on identifying gas zones from fizz-water. Russell et al. (2003) also used the parameter $\lambda\rho$ to extract the fluid component. Hedlin (2000) and Batzle et al. (2001) proposed the different combinations of petro-physics parameters to detect hydrocarbon.

Based on Russell et al.'s study (2003), Liu and Cong (2012) presented a new fluid factor which makes use of both Poisson impedance and the fluid factor

$\lambda\rho$ to reveal the potential of gas/oil reservoirs and illustrated a better effect on fluid identification.

Fluid elastic impedance (FEI) was introduced to discriminate fluid on the basis of Russell's approximation. Zhang et al. (2009) showed that inversion of FEI can be much helpful for fluid discrimination. Vasheghani and Lines (2012) applied rock physics model to estimate heavy oil viscosity by using crosswell seismic data. Most of the methods have been verified and applied to gas reservoirs (Hornby, 1998).

Pei et al. (2010) evaluated the sensitivity of different fluid identification factors by the fluid sensitivity indicator (FSI) to identify reservoir. Their study confirmed that the fluid factors which were selected by FSI are more sensitive than the AVO attributes in distinguishing hydrocarbon. However, the parameters yield by FSI methods shows a poor ability in low porosity reservoir. In this work, the relations between variations of rock physics parameters and fluid-saturation changes are investigated based on real data.

By considering the data distribution features on rock property crossplots, a quantitative evaluation method on fluid sensitivity of rock parameters is presented. The method is applied to the gas reservoirs from carbonates of Sichuan (southwest of China). The changes of fluid identification factors are calculated between the different fluid saturation states. Thirteen rock physics parameters are discussed in this study to analyze the properties of sediment rocks with different pore fluids.

FLUID SENSITIVITY INDICATOR

To quantitatively evaluate the parameter variations from the hydrocarbon (oil/gas) saturation to water (brine) saturation state, Pei et al (2010) introduced the fluid sensitivity indicator (FSI), which represent the relative variations when the saturation state changes. The evaluation indicator FSI is:

$$FSI = (\bar{X}_W - \bar{X}_H)/\bar{X}_H \quad , \tag{1}$$

where $\bar{X}_W$ and $\bar{X}_H$ are the mean values of rock physics parameters where the rocks are saturated with hydrocarbon (oil/gas) and water (brine), respectively. In this study, thirteen main fluid identification factors of rock physics parameters are analyzed. Among these parameters, V_P (P-wave velocity) and Z_P (P-wave impedance) are related to P-waves, V_S (S-wave velocity), Z_S (S-wave impedance), V_S/ρ and $\mu\rho$ are related to S-waves, and V_P/V_S, E (Young's modulus), ρ, λ, $\lambda\rho$, ν (Poisson's ratio), $\lambda+\mu$ are related to both P- and S-waves.

Different parameters and their combinations will have different fluid sensitivities. Usually, the parameter with greater value of FSI indicates the higher sensitivity of fluid identification.The fluid sensitivity of parameters evaluated by FSI has been verified by the crossplot technique and guided seismic AVO pre-stack inversion (Pei et al., 2010). Also Pei stated that a single fluid identification factor evaluated by FSI may be ineffective for fluid discrimination if the original data have poor signal-to-noise ratio.

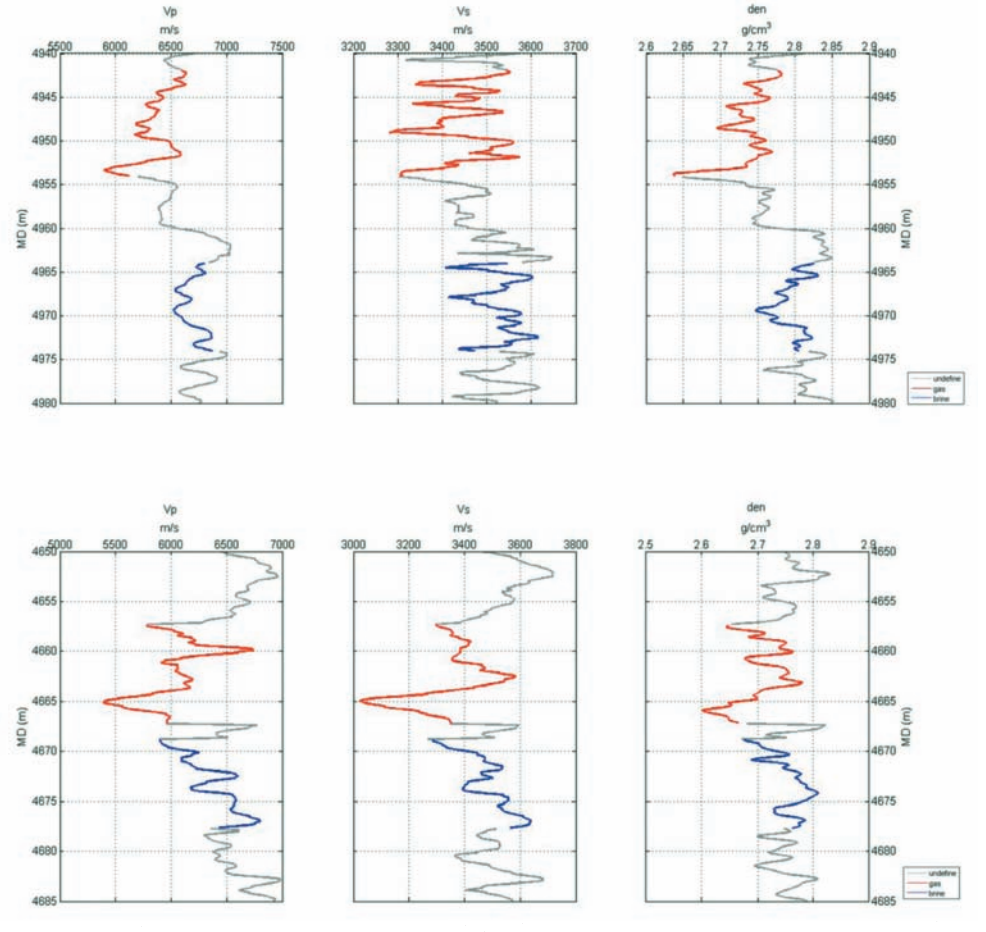

Fig. 1. Gas- and brine-saturated rocks in logging data (P-wave velocity, S-wave velocity and density) from well A (a) and well B (b). Red indicates the gas-saturated rocks and blue indicates the brine-saturated rocks.

EFFECTIVE FLUID SENSITIVITY INDICATOR (EFSI)

As we have discussed above, usually parameters with higher FSI values are more sensitive to fluid state changes, but it does not work for all situations. This can be demonstrated with the real logging data from the two wells of a gas field from middle Sichuan basin (southwest of China). The reservoir rocks are mainly dolomites (with rare clay) which are saturated with gas and brine, and the brine-saturation is in the range of 0-100%. The dolomite reservoirs have low porosity and low permeability. The burial depth of the target layer is 4535-4775 meters from the earth's surface, and the thickness of the strata is around 80-100 meters. Most of the pores in reservoir rocks are dissolved pores and cracks, and the intergranular pores are very common in the strata.

Two datasets from the two different wells are show in Fig. 1. Both datasets contain gas-saturated and brine-saturated samples. The average values of the rock physics parameters from the two datasets are close. But the statistical distributions patterns are not the same.

Similar average values of the rock physics parameters lead to similar FSI values as is shown in Table 1 and Fig. 2. Though FSI values of the two groups are very close, their fluid identification capabilities are different. As is shown in Fig. 3, in crossplots of well A, the data symbols can be clearly divided into the two categories with different fluid saturation by a dashed line, while for the data points of well B, the two states cannot be discriminated easily.

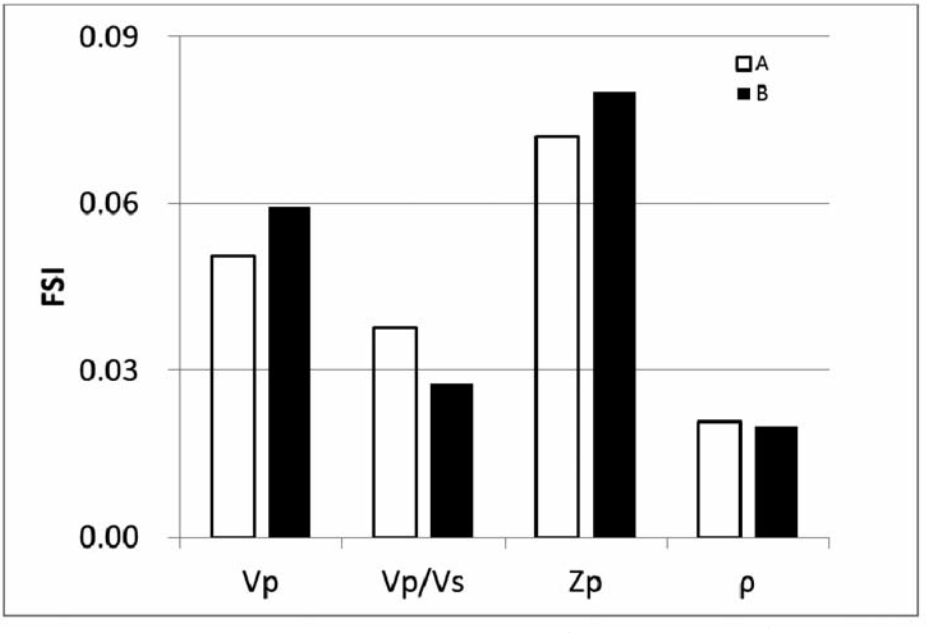

Fig. 2. FSI values of well A and well B.

Table 1. FSI, CD and EFSI of the gas- and brine-saturated rocks from well A and well B.

		V_P	V_P/V_S	Z_P	ρ
Well A	FSI	0.050483	0.037602	0.072067	0.020683
	CD	0.022364	0.017971	0.029827	0.009181
	EFSI	2.257295	2.092318	2.416196	2.252829
Well B	FSI	0.059264	0.027542	0.080098	0.019891
	CD	0.043427	0.02666	0.054017	0.014807
	EFSI	1.364682	1.033088	1.482847	1.343313

From the statistical point of view, two sets of samples with the same average value may have very different distribution patterns. To determine the fluid identification sensitivity of a specific parameter, the averages and distribution patterns should both be taken into account.

As is shown in Fig. 2, Figs. 3b and 3d, the optimized parameters of FSI are not so efficient for discriminating fluid in the rocks from well B, since FSI only considers only the relative variation between the averages. Thus a coefficient of dispersion is introduced to analyze the distribution ranges of the data of rock physics parameters. The CD can be expressed as the following equation:

$$CD = (SD_O/\bar{X}_H + SD_W/\bar{X}_W)/2 \quad , \tag{2}$$

where SD_O and SD_W are the standard deviations (SD) of the parameters of gas- and brine-saturated rocks, respectively. A low CD indicates that the data points tend to be distributed very close around the mean value. A high CD indicates that the data points are sparsely distributed in a larger range.

Considering the influence of CD, we suggest a new expression to identify pore fluid sensitivity of the rock parameters. The new indication factor of effective fluid sensitivity (EFSI) is defined as:

$$EFSI = FSI / CD \quad . \tag{3}$$

Even with the same FSI, a smaller value of CD produces a larger EFSI, which means a higher ability of fluid detection. Rock physics parameters cannot

be employed to identify pore fluid directly when their EFSI are smaller than or equal to 1. Because in this case, their relative variations from oil(gas)-saturated to brine-saturated states are less than or equivalent to the dispersion effect. Parameter whose EFSI is larger than 1 can be applied to fluid indication. The larger value of EFSI shows the higher efficiency.

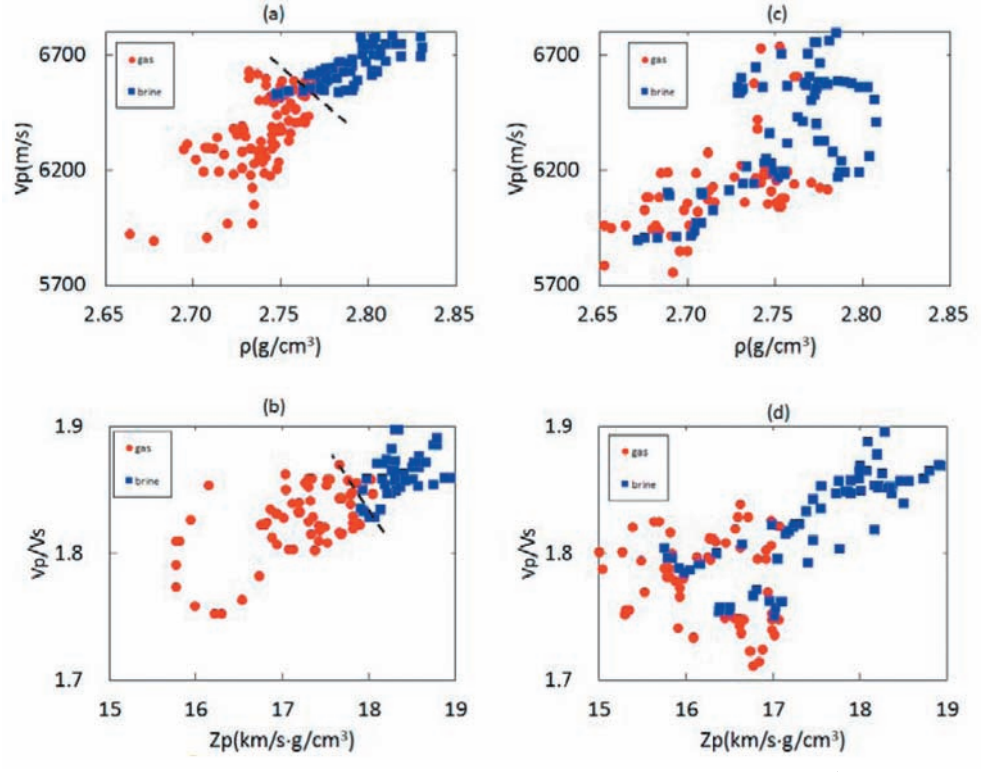

Fig. 3. Crossplots of the two well data with the close FSI values but different EFSI. (a, b) The gas-saturated and brine-saturated samples of well A can be clearly separated; (c, d) The samples of well B cannot be separated clearly.

EFSI is utilized instead of FSI, and the phenomena in Fig. 3 can be easily explained. As is shown in Fig. 4, well A has a larger EFSI value than well B, which means that samples in well A are much easier to be discriminated with fluid-saturation states. When the gas-saturated and brine-saturated data points are blended together, FSI cannot give an accurate evaluation of fluid sensitivity of rock physics parameters. The EFSI which takes the data distribution into

account can be much more efficient in selecting the best rock parameters to discriminate the gas-saturated samples from brine-saturated ones.

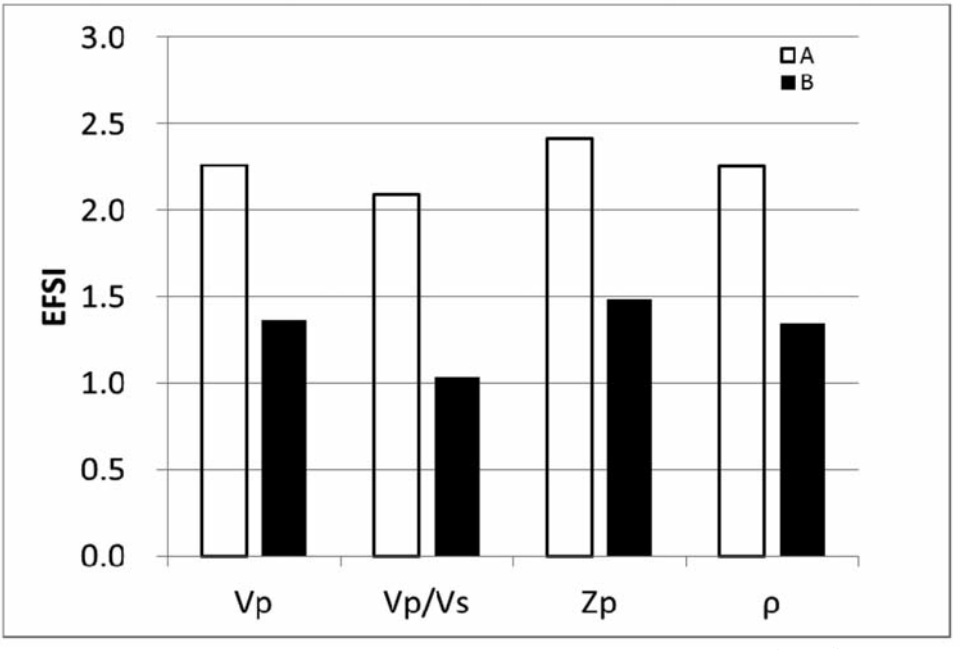

Fig. 4. EFSI values of well A and well B.

EXAMPLE OF CARBONATE HYDROCARBON RESERVOIR IDENTIFICATION

In the example, logging data from the well of middle Sichuan basin (southwest of China) are analyzed. We select another well (well 23) from the same gas field, which is located beside a seismic test line. P-wave velocity measurements range (Fig. 5) from 5500 m/s to 7100 m/s for the reservoir rocks. For S-wave velocities, the measurements are in range of 3000 - 3600 m/s. The measured densities in the target strata are in range of 2.6 - 2.85 g/cm^3.

Table 2 shows the $\bar{X}$, SD, FSI, CD and EFSI values. FSI, CD and EFSI of the thirteen rock physics parameters are calculated from eqs. (1)-(3). Fig. 6 compares the FSI and EFSI results of the parameters. And the thirteen parameters can be classified into the four types (Fig. 7):

- Type 1: Low FSI and low EFSI, for instance, V_S, Z_S and V_S/ρ;
- Type 2: High FSI but low EFSI, for instance, E and $\mu\rho$;

- Type 3: Low FSI but high EFSI, for instance, V_P/V_S and ρ;
- Type 4: High FSI and high EFSI, including V_P, Z_P, λ, $\lambda\rho$, v and $\lambda+\mu$.

The Type 1 parameters have lower FSI and EFSI results than the average level and cannot be used to identify pore fluid. Parameters of the Type 4 show good ability in fluid identification with both high FSI and EFSI values. Attentions also should be paid on the identification difference of the fluid factors selected by EFSI and FSI.

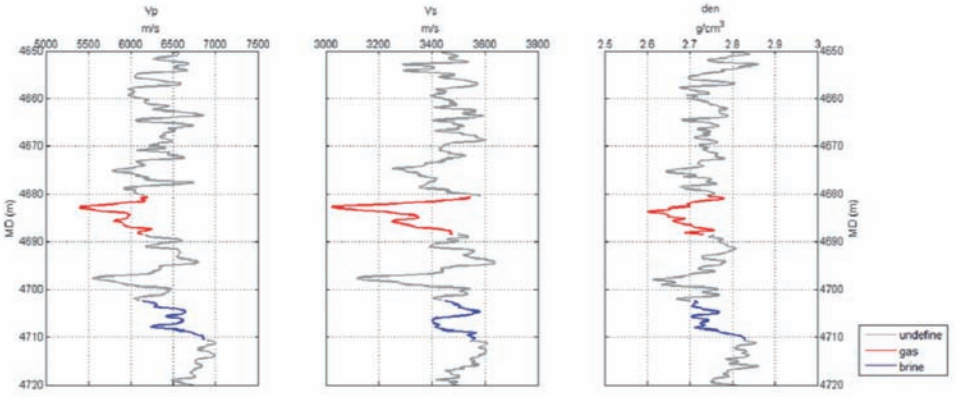

Fig. 5. V_P, V_S and density logging curves of well 23. Red indicates the gas-saturated rocks and blue indicates the brine-saturated rocks.

Table 2. $\bar{X}$ and SD pairs of gas and brine reservoir samples. FSI, CD, and EFSI of the thirteen rock physics parameters.

		Vp (km/s)	*Zp* (km/s·g/cm)	*λ* (GPa)	*v*	*λρ* (GPa·g/cm^3)	*λ+μ* (GPa)	*ρ* (g/cm^3)	*Vp/Vs*	*E* (GPa)	*μρ* (GPa·g/cm^3)	*Vs* (km/s)	*Vs/ρ* (km·cm^3/s·g)	*Zs* (km/s·g/cm^3)
$\bar{X}$	*gas*	5.908	15.893	64.585	0.272	173.830	94.074	2.689	1.787	74.987	79.383	3.307	1.230	8.897
	brine	6.533	17.941	83.916	0.300	230.637	117.349	2.745	1.873	86.910	91.830	3.489	1.271	9.579
SD	*gas*	0.225	0.791	5.478	0.007	16.850	8.099	0.044	0.019	6.797	8.448	0.135	0.040	0.474
	brine	0.266	0.999	11.612	0.017	35.172	12.359	0.044	0.058	4.728	5.475	0.050	0.011	0.291
FSI		0.057	0.081	0.183	0.087	0.203	0.142	0.025	0.044	0.069	0.075	0.013	0.013	0.038
CD		0.039	0.053	0.112	0.041	0.125	0.096	0.016	0.021	0.073	0.083	0.028	0.020	0.042
EFSI		1.448	1.532	1.640	2.096	1.631	1.485	1.566	2.113	0.955	0.898	0.457	0.616	0.915

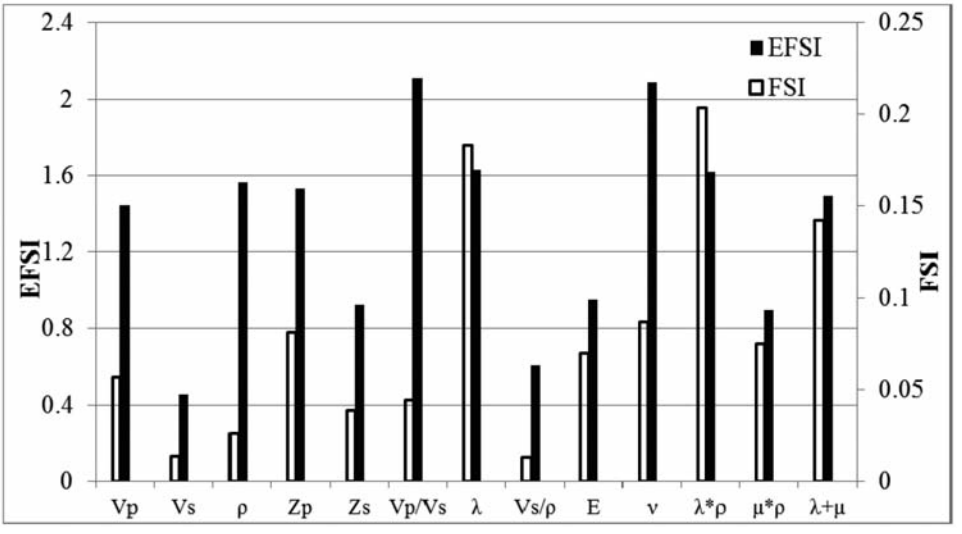

Fig. 6. The FSI and EFSI results of the rock physics parameters of well 23.

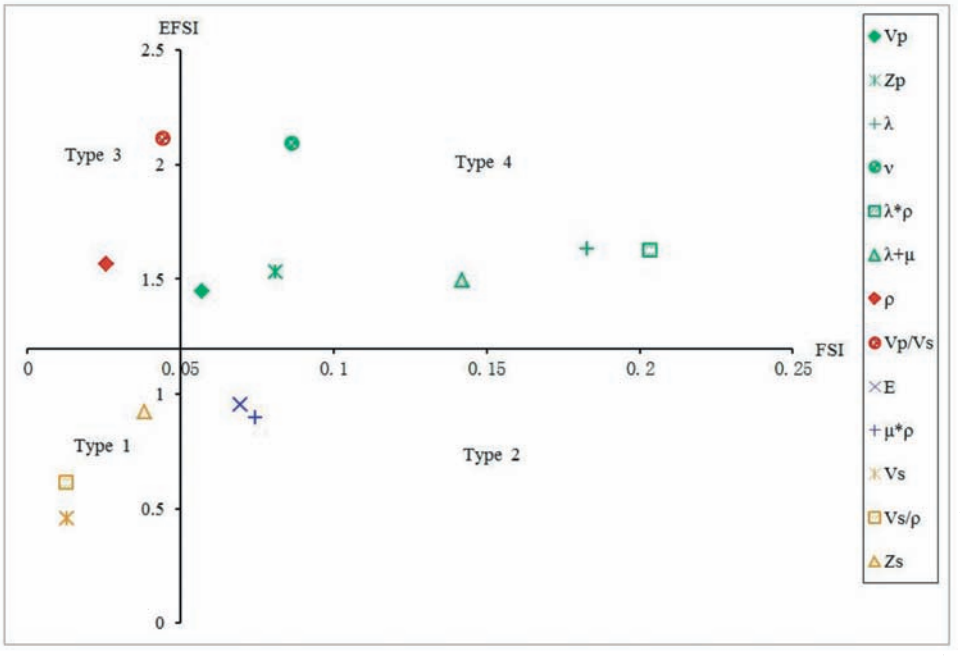

Fig. 7. The thirteen rock physics parameters of the four types.

Some of the data with different fluid saturation states are mixed together (see Fig. 8) and the boundary between gas-saturated and brine-saturated ones are not evident. For the further study on the discriminability of fluid in crossplots, clustering analysis is employed to quantitatively estimate the overlapping degree in crossplots, which we called OR (Appendix). The range of OR is valued in 0-100%. The two groups of data can be perfectly distinguished when the OR is close to 0, while the two groups are deeply mixed when the OR approaches 100%. A parameter with less overlaps gets higher ability of fluid identification.

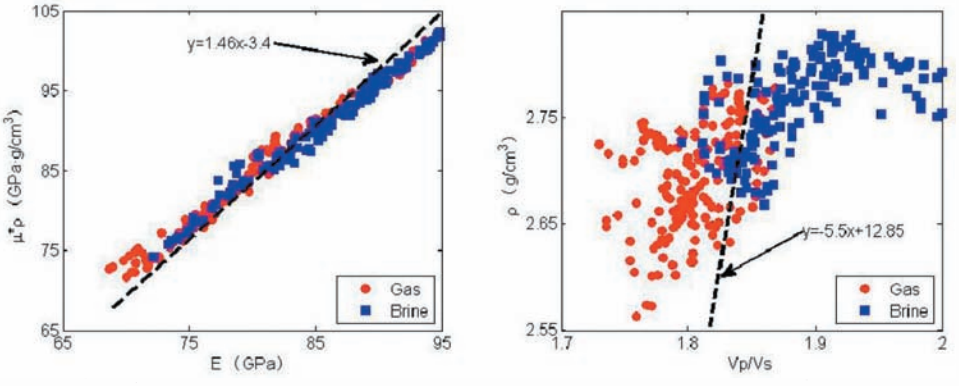

Fig. 8. Crossplots of the rock physics parameters of the carbonate reservoirs. (a) Crossplot 5 with the Type 2 parameters; (b) Crossplot with the Type 3 parameters. The dash lines are the separating lines to make minimum OR.

If the Type 2 parameters with high FSI but low EFSI values are used for crossplot analysis, as is shown in Fig. 8a, the data points of gas-saturated and brine-saturated reservoirs are mixed. The quantitative analysis shows the overlap of the crossplot in Fig. 8a is 46.6%. The parameters used in Fig. 8b are both Type 3 (low FSI and high EFSI values). The overlap of Fig. 8b is 8.7%, and the improvement is 37.9% from Fig. 8a, which means it will be much more favorable for the further applications of hydrocarbon seismic identification.

It is illustrated in Fig. 9, the crossplots with the parameters of different types. In Fig. 9a Type 2 and Type 4 are used. The calculated overlap is 12.5%. In Fig. 9b Type 3 and Type 4 are used, and the OR is 9.2%. In the case that the Type 4 parameter is employed, which is shown in Figs. 9a and 9b crossplots, the OR in the crossplot with the Type 3 parameter is 3.3% less than that with the Type 2.

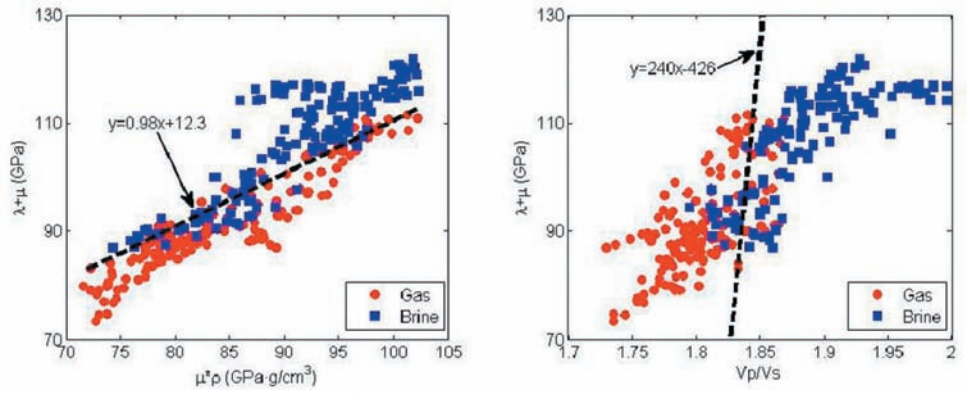

Fig. 9. Crossplots of the rock physics parameters of carbonate reservoirs. (a) Crossplot 15 with the Type 2 and Type 4 parameters; (b) Crossplot with the Type 3 and Type 4 parameters.

DISCUSSION

By considering that the parameters v and V_P/V_S are actually redundant to each other, their sensitivities to fluid should be the same. However, the FSI of v is twice the FSI of V_P/V_S (Fig. 6). EFSI takes the data dispersion effect into account so that the scale of the parameters will not impact on fluid sensitivity analysis. For instance, $\mu\rho$ is the square of Z_S, and the FSI of $\mu\rho$ is almost twice that of Z_S, however, by using EFSI evaluation method, the sensitivities to fluid for the two parameters are completely identical.

Fig. 10 illustrates the pre-stack seismic inversion results of the rock physics parameters around well 23. Based on the gas production test report of well 23, four markers are overlaid on the seismic inversion section: A-TOP and A-BOT stand for the top and bottom of the gas layer A, and B-TOP and B-BOT represent the boundaries of the brine-saturated layer B, respectively. In Fig. 10a, the seismic inversion result of V_P/V_S matches the markers very well, where gas and brine layers could be easily distinguished. In the inversion results of $\mu\rho$ of Fig. 8b, the $\mu\rho$ results of the gas layer and brine layer are almost the same, although the two layers of reservoirs can be identified from non-reservoir rocks.

The parameter V_P/V_S has high EFSI but low FSI values (Type 3), while $\mu\rho$ has high FSI but low EFSI values (Type 2). The seismic inversion profile has shown that the parameter V_P/V_S is proved to be a better parameter for the purpose of gas identification.

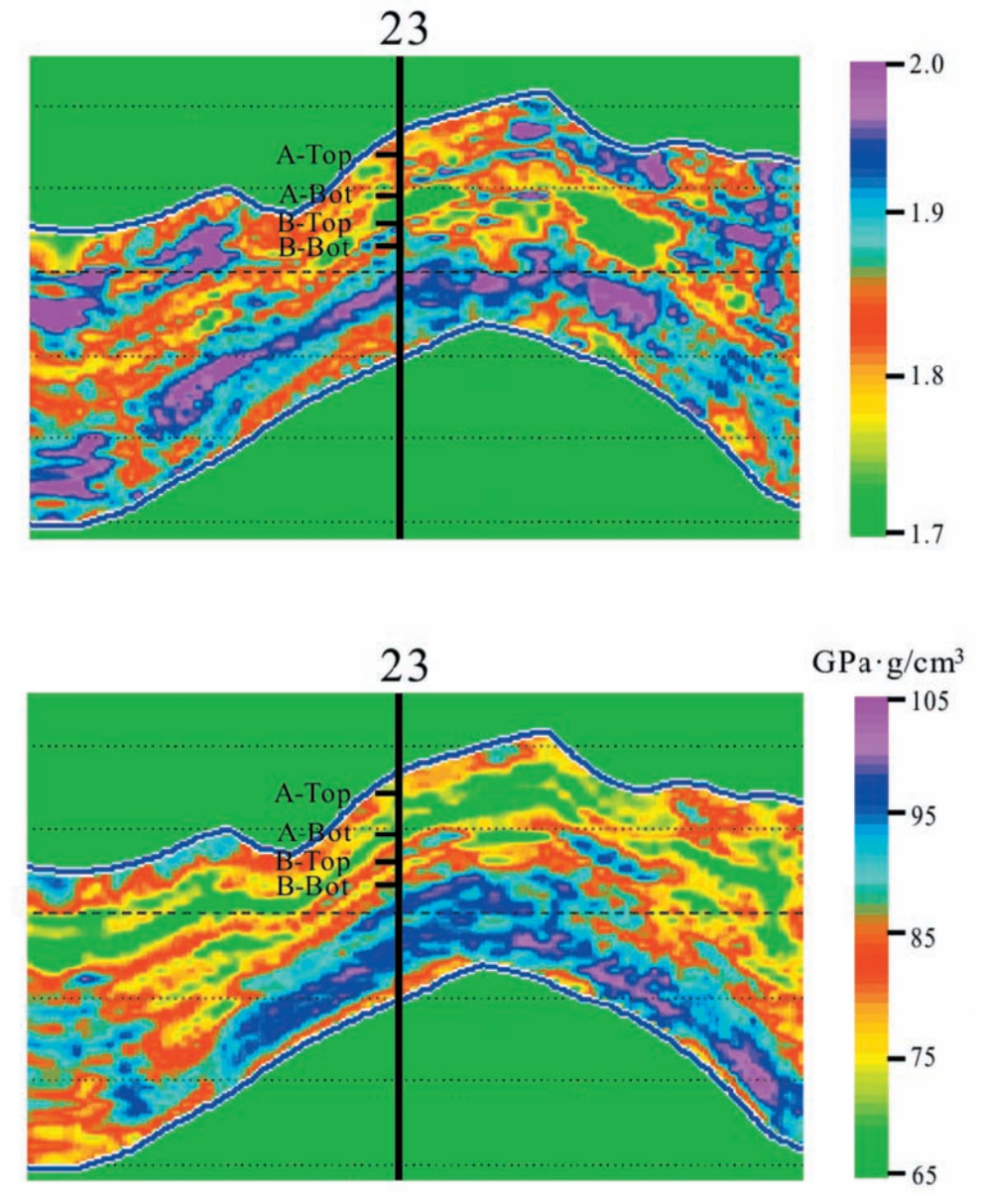

Fig. 10. The seismic inversion profiles. (a) Inversion results of V_P/V_S; (b) Inversion results of $\mu\rho$. A-TOP and A-BOT are the top and bottom of a gas layer A, respectively. B-TOP and B-BOT are the top and bottom of a brine-saturated layer B, respectively.

CONCLUSION

In this study, an optimized indicator EFSI is proposed to quantitatively evaluate the effect of pore fluid changes on rock physics parameters. We demonstrate the limitation of the indicator FSI from the real datasets. Thus the approach of EFSI is introduced, which not only considers the variations of the mean values of rock physics parameters between different saturated states, but also analyzes the distribution patterns of the data on crossplots with different fluids. From a statistical point of view, EFSI is more effective than FSI to evaluate the fluid sensitivity of rock physics parameters.

EFSI approach is successfully implemented on the real data examples, and well-log data and seismic data are analyzed. The method of overlap analysis is introduced to quantitatively evaluate the ability of rock parameters in fluid identification on crossplots. The example shows that rock physics parameters selected by the EFSI approach have better fluid-sensitivity than those selected by FSI. EFSI evaluation can help sorting out the most effective rock physics parameters and guides hydrocarbon identification in seismic exploration and production.

ACKNOWLEDGEMENTS

This study is supported by the Distinguished Professor Program of Jiangsu Province and the National Science and Technology Major Project of China (2011ZX05013-001).

REFERENCES

Agersborg, R., Johansen, T.A. and Ruud, B.O., 2008. Modeling reflection signatures of pore fluid and dual porosity in carbonate reservoirs. J. Seismic Explor., 17: 63-83.

Avseth, P., 2000. Combining Rock Physics and Sedimentology for Seismic Reservoir Characterization of North Sea Turbidite Systems. Ph.D. thesis, Stanford University.

Batzle, M. and Wang, Z., 1992. Seismic properties of pore fluids. Geophysics, 57: 1396-1408.

Batzle, M., Han, D. and Hofmann, R., 2001. Optimal hydrocarbon indicators. Expanded Abstr., 71st Ann. Internat. SEG Mtg., San Antonio: 1697-1700.

Castagna, J.P. and Smith, S.W., 1994. Comparison of AVO indicators: A modeling study. Geophysics, 59: 1849-1855.

Dillon, L., Schwedersky, G., Guilherme, V., Velloso, R. and Numes, C., 2003. A multiscale 35 DHI elastic attributes evaluation. The Leading Edge, 22: 1024-1029.

Fatti, J.L., Smith, G.C., Vail, P.J., Strauss, P.J. and Levitt, P.R., 1994. Detection of gas in sandstone reservoirs using AVO analysis: A 3-D seismic case history using the Geo-stack technique. Geophysics, 59: 1362-1376.

Gray, D., Goodway, B. and Chen, T., 1999. Bridging the gap: using AVO to detect changes in fundamental elastic constants. Expanded Abstr., 61st EAGE Conf., Helsinki: 6-50.

Goodway, W., Chen, T. and Downton, J., 1997. Improved AVO fluid detection and lithology discrimination using Lamé petrophysical parameters. Expanded Abstr., 67th Ann. Internat. SEG Mtg., Dallas: 183-186.

Goodway, W., 2001. AVO and Lamé constants for rock parameterization and fluid detection. Recorder, 26: 39-60.

Guo, Y., Ma, H., Ba, J., Zhao, H., Long, C. and Wang, H., 2014. Fluid sensitivity of rock physics parameters in sandstone, quantitative analysis. Extended Abstr., 76th EAGE Conf., Amsterdam: P11 09.

Guo, Y., Ba, J., Zhao, H., Dovrkin, J., Yao, F. and Hu, T., 2013. Velocity dispersion in sandstones with oil and brine: Experimental measurements and theoretical predictions. Extended Abstr., EAGE Workshop on Seismic Attenuation, Singapore.

Hedlin, K., 2000, Pore space modulus and extraction using AVO. Expanded Abstr., 70th Ann. Internat. SEG Mtg., Calgary, AB: 170-173.

Hilterman, F.J., 2001. Seismic Amplitude Interpretation. 2001 distinguished instructor short course, No. 4. SEG, Tulsa, OK.

Hornby, B.E., 1998. Experimental laboratory determination of the dynamic elastic properties of wet drained shakes. Geophys. Res., 103: 945-964.

Imhof, M.G., 2003. Estimating reservoir changes from AVO changes. J. Seismic Explor., 12: 141-150.

Keho, T.H., 2000. The AVO hodogram: Using polarization to identify anomalies. Expanded Abstr., 70th Ann. Internat. SEG Mtg., Calgary, AB: 118-121.

Keho, T.H., Lemanski, S., Ripple, R. and Tambunan, B.R., 2001. The AVO hodogram: Using polarization to identify anomalies. The Leading Edge, 20: 1214-1224.

Liu, M. and Cong, T., 2012. Fluid discrimination using a new fluid-identifying factor. Expanded Abstr., 82nd Ann. Internat. SEG Mtg., Las Vegas: 1-5.

Mavko, G., Mukerji, T. and Dvorkin, J., 2009. The Rock Physics Handbook: Tools for Seismic Analysis of Porous Media (2nd ed.). Cambridge University Press, Cambridge.

Ostrander, W.J., 1984. Elastic waves through a packing of spheres. Geophysics, 59: 1362-1376.

Pei, F., Zou, C., He, T., Shi, G., Qiu, G. and Ren, K., 2010. Fluid sensitivity study of elastic parameters in low-medium porosity and permeability reservoir rocks. Appl. Geophys., 7: 1-9.

Russell, B.H., Hedlin, K., Hilterman, F.J. and Lines, L.R., 2003. Fluid-property discrimination with AVO: A Biot-Gassmann perspective. Geophysics, 68: 29-39.

Shaw, R.K. and Sen, M.K., 2006. Use of AVOA data to estimate fluid indicator in a vertically fractured medium. Geophysics, 71(3), C15-C24.

Simm, R., White, R. and Uden, R., 2000. The anatomy of AVO crossplots. The Leading Edge, 2: 150-155.

Smith, G.C., 2003. The fluid factor angle and the crossplot angle. Expanded Abstr., 73rd Ann. Internat. SEG Mtg., Dallas: 185-188.

Smith, G.C., 2000. A comparison of the fluid factor with λ and μ in AVO analysis. Expanded Abstr., 70th Ann. Internat. SEG Mtg., Calgary, AB: 122-125.

Smith, G.C. and Sutherland, R.A., 1996. The fluid factor as an AVO indicator. Geophysics, 61: 1425-1428.

Vasheghani, F. and Lines, L.R., 2012. Estimating heavy oil viscosity from crosswell seismic data. J. Seismic Explor., 21: 247-266.

Zhang, S., Yin, X. and Zhang, F., 2009. Fluid discrimination study from fluid elastic impedance. Expanded Abstr., 79th Ann. Internat. SEG Mtg., Houston: 2437-2441.

Zhou, Z. and Hilterman, F.J., 2007. Is there a basis for AVO attributes? Expanded Abstr., 77th Ann. Internat. SEG Mtg., San Antonio: 244-248.

Zhou, Z., and Hilterman, F. J., 2010, A comparison between methods that discriminate fluid content in unconsolidated sandstone reservoirs, Geophysics, 75(1), B47-B48.

APPENDIX

CLUSTERING ANALYSIS OF OVERLAPPING

In the example of gas reservoirs, clustering analysis of overlap ratio (OR) was applied to quantitatively estimate the discriminability of data of two different states, which can be described by the following equation:

$$\text{overlap}(a,b) = \sum_{m} \text{dist}(\text{Error}_m,a,b) \,/\, \sum_{n} \text{dist}(\text{Data}_n,a,b) \quad , \tag{A-1}$$

where a and b are the parameters determining a line $y = ax + b$. Error_m is the set of data points which are located at the wrong side of the line (Generally, the two sides of the line on crossplots indicate the two different saturation states. Some data points which are located on the one side of the line where most of the other points have got a different saturation state are taken as Error_m), while Data_n is the set of all data points. In eq. (A-1), $\Sigma_m\text{dist}(\text{Error}_m,a,b)$ is the sum of the distance between Error_m and the separation line, and $\Sigma_n\text{dist}(\text{Data}_n,a,b)$ is the sum of the distance between all the data points and the line.

To find the best line with the minimum overlap, the method of linear fitting and linear regression is applied as a starting point. Then the iteration is implemented with a following objective function:

$$F = \text{Min}[\text{overlap}(a,b)] \quad . \tag{A-2}$$

For a certain crossplot with a line $y = ax + b$, eq. (A-1) is used to calculate the value of "*overlap*". By changing a and b values, we search all the possible lines, until a global minimum of this objective function is reached. The optimized line is called the "*separating line*". The separating line and OR are the indicators evaluating the discriminability of two data groups.